



## FRACTURE IDENTIFICATION OF STEEL STRUCTURES FROM WAVEFORMS USING CONVOLUTIONAL NEURAL NETWORKS

X. Wang<sup>(1)</sup>, L.Y. Wang<sup>(2)</sup>, and J. Dang<sup>(3)</sup>

(1) Assistant Professor, Tokyo University of Science, Noda, Japan. wangxin@rs.tus.ac.jp

(2) Graduated Student, Saitama University, Saitama, Japan. o.r.984@ms.saitama-u.ac.jp

(3) Assistant Professor, Saitama University, Saitama, Japan. dangji@mail.saitama-u.ac.jp

### **Abstract**

After destructive earthquakes, rapid decision making, such as continuous use, reinforcement, demolition is very essential. Therefore, reliable information of structural damage is indispensable. For steel building structures, fractures at beam ends are very crucial, because it is the criteria to judge a structure is possible to be reinforced or not. As a result of the beam-end fractures, the story shear rigidity will be reduced. Conventionally, as an approach of structural health monitoring, beam-end fractures can be speculated from the decrease of the natural frequencies and the increase of shear-wave travel time within stories based on vibration measurement, such as ambient noise and earthquake responses. However, for the detection of beam-end damages, not only its occurrence but also the locations should be indicated for the implementation of reinforcement.

Based on vibration measurement of shake-table tests of steel structures, we realized that it is possible to detect the beam-end fractures directly from the waveforms through recognizing the pulse-like shock waves generated by beam-end fractures. However, it is time-costly and less reliable to visually recognize the shock waves from the waveforms. With the development of deep learning method, the Convolutional Neural Networks (CNNs) have been proved as one of the effective methods for feature extraction from data.

In this study, a direct approach to detect beam-end fracture from acceleration waveforms is proposed using a CNN model. The large amount of training data (20,000) was generated by nonlinear response analysis of single-degree-of-freedom models with changing periods from 0.3 sec to 2 sec. The input motions were randomly chosen from 18 motions in the aseismic design code of Japan. In order to simulate the real vibration condition, noise was added to the simulated waveforms. Half of the ambient-noise-added data was used as training data "with no beam-end fracture". The other half of the data were used as the training data "with beam-end fracture data" by adding shock waves, the shapes of which were similar to the records of shake-table tests. The trained CNN model was validated using acceleration waveforms recorded during the shake-table tests of an 18-story and a 3-story steel frame building. As a result, the proposed CNN model can detect the beam-end fractures with high accuracy. That is to say the proposed CNN model is sensitive to the sudden and drastically changes in acceleration waveforms and can correctly identify the feature of beam-end fractures.

*Keywords: Beam-end fracture detection, Convolutional Neural Network, acceleration waveforms, shake-table test*



## 1. Introduction

During the 1995 Great Hanshin Earthquake, Japan, 104,004 building structures were completely destroyed and 136,952 building structures were partially destroyed<sup>[1]</sup>. It was the first time in Japan confirmed the beam-end fracture occurred at beam-column joints of steel frame building structures. And it is worth noting that even the beam-end fractures have occurred the visual damages were slight<sup>[2]</sup>.

Generally, there are four stages of the performance of a building structure under earthquakes: (1) Elastic responses (undamaged); (2) Elastoplastic responses (no residual deformation); (3) Structural damage, such as beam-end fractures and bulking of columns (residual deformation); (4) Collapse<sup>[3]</sup>. From the seismic safety perspective, the judgement of risk of collapse is very important. The collapse caused by the progression of fractures occur at beam ends, especially the lower flange of the beams. The beam-end fractures deteriorate the shear rigidity of the stories. Therefore, the quick detection of the beam-end fracture for building structures after earthquake are very important. However, it is difficult to recognize this kind of damages by visual inspection.

From the shake-table tests of steel building structures performed by the full-scale three-dimensional vibration destruction test facility E-Defense (National Research Institute for Earth Science and Disaster Prevention), it is realized that the beam-end fractures can be recognized directly from the shock waves in the acceleration waveforms which were recorded near the column-beam connections. However, it is time costly and error-prone to recognize the shock waves by visual inspection. Recently, with the development of neural network technique, it is possible to extract the features of shock waves generated by beam-end fractures automatically.

In this study, we proposed a Convolutional Neural Networks (CNN) model to detect the beam-end fractures directly from acceleration waveform without analyses of records. The big amount (20,000) of training data were prepared using numerical simulation of responses of non-linear single-degree-of-freedom models with changing periods in the range of 0.3 sec to 2 sec under the input motions which were randomly chosen from 18 motions in the aseismic design code of Japan. The shock waves picked out from the shake-table tests of a 1/3-scale specimen of an 18-story steel building structure were added to half of the simulated acceleration response waveforms (10,000) to generate the waveforms with beam-end fractures. The other half of the data were used as without beam-end fractures. The proposed CNN model can extract features from acceleration waveform recorded by sensor without any filter, which means the raw data can be used directly without any complicated data processing and modelling assumptions.

## 2. Shock waves caused by beam-end fracture

### 2.1 Outlines of two shake-table test of steel building structure

Experiment A was an experiment conducted in December 2013 to verify the collapse capacity of a steel-frame high-rise building using a 1/3-scale specimen of an 18-story steel building structure<sup>[4]</sup>. Figure 1 (a) shows a photograph of the test specimen and the location of the seismometers. The input ground motion was a long-period ground motion with a hypocenter of the Nankai Trough of Japan assuming a three-way linkage of Tokai, Tonankai, and Nankai. The level of the input seismic motion was gradually increased, and excitation was performed from the elastic state to the collapse. The test specimen subjected to repeated vibrations was shaken by 2.2 times the design value, and the columns and beams on the lower floor were damaged. In this study, we used the acceleration waveform recorded by a seismograph (filled square in Fig. 1) installed near the connections of columns and the beams where the beam-end fracture occurred.

Experiment B is an experimental study on seismic safety examination for a 3-story steel building<sup>[2]</sup>. Figure 1 (b) shows a photograph of the test specimen and the location of the seismometer. The ground motion used for the excitation was the NS component of the acceleration waveform observed at JR Takatori Station during the 1995 Hyogoken-Nanbu Earthquake.

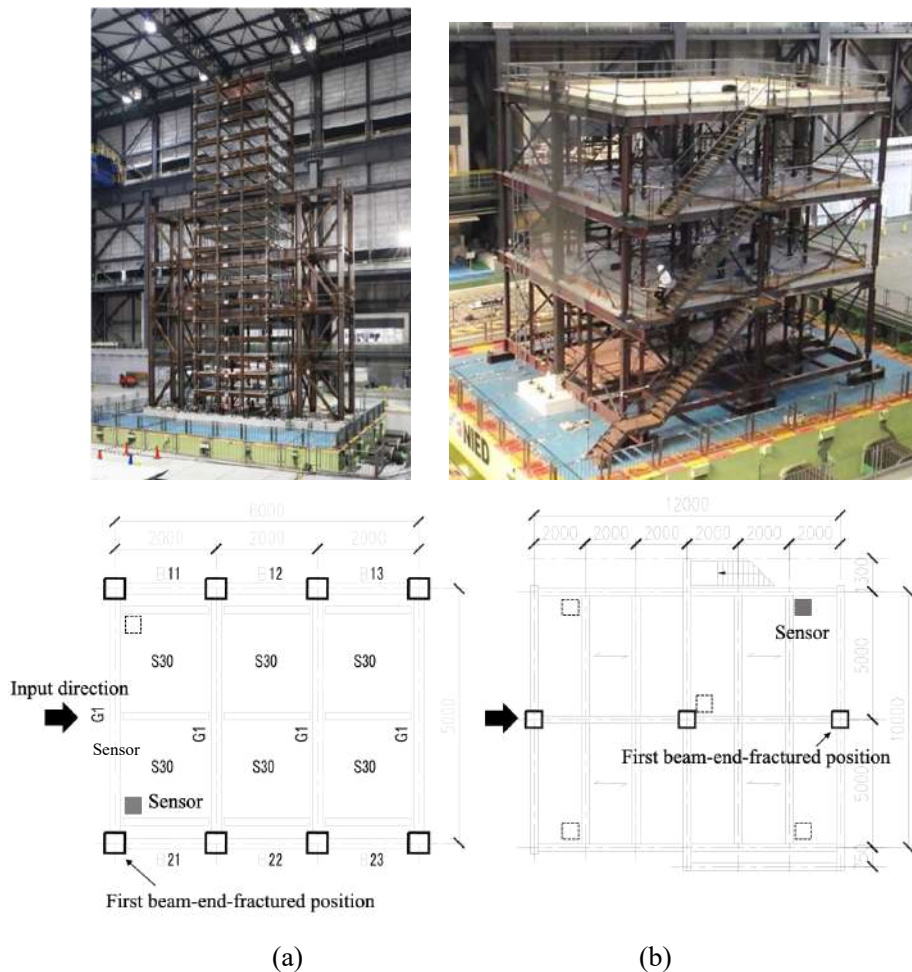


Fig. 1 (a) 1/3-scale specimen of an 18-story building and locations of seismometers; (b) Actual size specimen of a 3-story building and locations of seismometers.

## 2.2 Analysis of noise in waveforms

Fig. 2 shows the input motions and the response acceleration waveforms recorded near the connections where the beam-end fracture occurred in shaking-table test A and B. Before extracting the shock waves due to the beam-end fractures, noises generated by environmental vibrations, human activities, measuring instruments, etc. mixed into the acceleration records were analyzed. The moving average of acceleration data was performed. And the difference between the original data and the data after the moving average was calculated. Fig. 3 shows an example of the comparison of 2-sec waveforms between the original data and that after the moving average. Fig. 4 shows the examples of two-sec noise waveform, the frequency of the noise amplitude, and the cumulative distribution function. The frequency of the noise amplitude was considered to be a normal distribution, and the maximum value of the noise amplitude generated with a 95% probability was found to be  $0.20 \text{ m/s}^2$  of shake-table test A and  $0.06 \text{ m/s}^2$  of shake-table test B.

## 2.3 Characteristics of shock waves caused by beam-end fracture

As shown in Fig. 5, it can be seen that there is a big change of the acceleration distribution with the height due to the shock waves generated by beam-end fracture. Using this phenomenon, the time when the beam-end fracture has occurred can be determined. Based on the wave shown in Fig. 2, the beam-end fracture occurred at 66.805 s in shake-table test A and 14.741 s in shake-table test B. Fig. 6 shows examples of



acceleration waveforms and damage photographs before and after the beam-end fracture occurred. The shock wave of the beam-end fracture is clearly visible in the acceleration waveform.

In order to quantify the magnitude of the shock waves generated by the beam-end fractures by the ratio of noise to signal, the data with length of 0.1 s before and after the beam-end fracture were extracted. The extracted motion waves are shown in Fig. 7. In this example, the ratio of the maximum amplitude of the shock waves to the maximum amplitude of the signal is  $9.117 / 6.309 = 1.45$  for shake-table test A and  $23.519 / 9.320 = 2.52$  for shake-table test B.

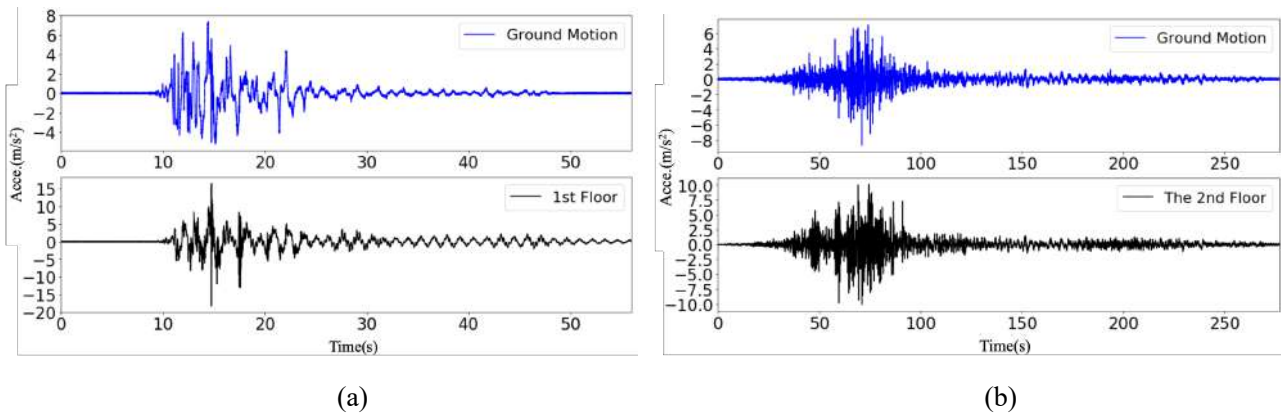


Fig. 2 Input motions and response acceleration waveforms of (a) experiment A and (b) experiment B.

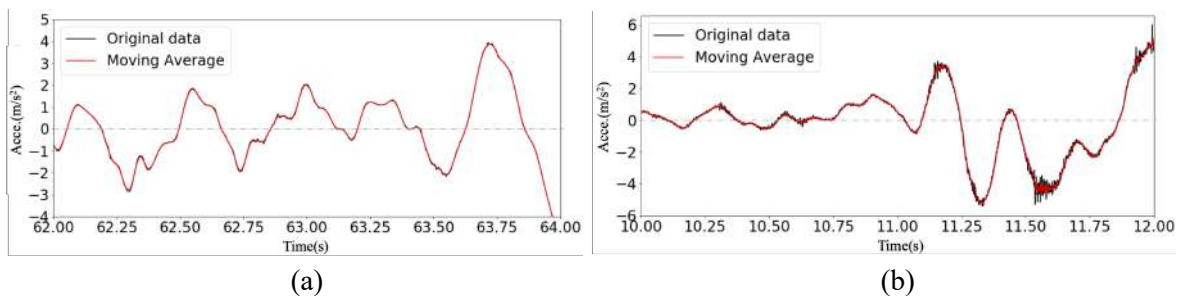


Fig. 3 Comparison of 2-sec waveforms between the original data and that after the moving average of (a) shake-table test A and (b) shake-table test B.

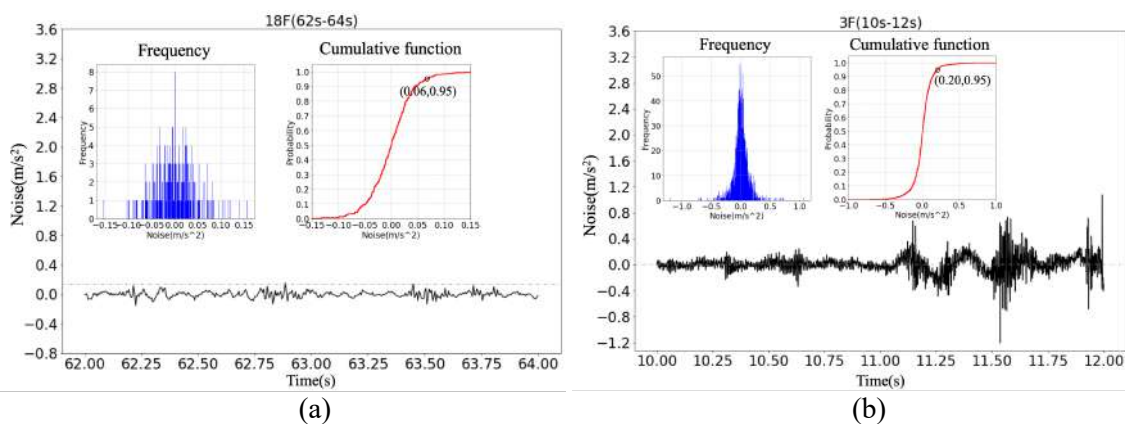


Fig. 4 Two-sec noise waveforms and noise quantification analysis results of (a) shaking table A and (b) shake-table test B.

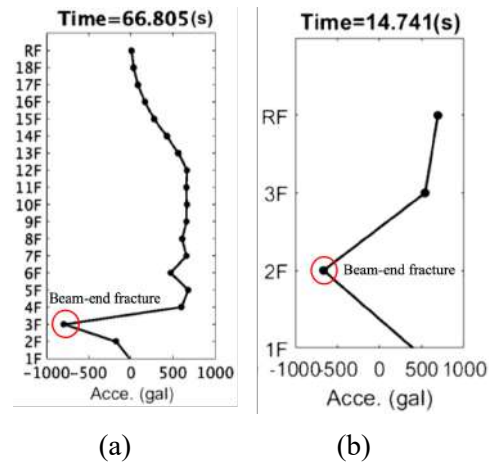


Fig. 5 Dramatic changes of the acceleration distribution with the height due to the shock waves generated by beam-end fracture in (a) shake-table test A and (b) shake-table test B.

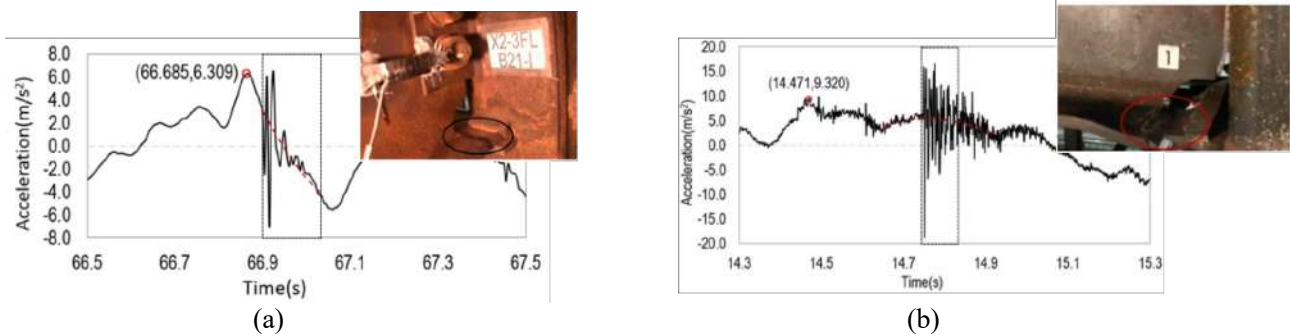


Fig. 6 Examples of waveforms generated by the beam-end fracture and corresponding damage photos in (a) shake-table test A and (b) shake-table test B.

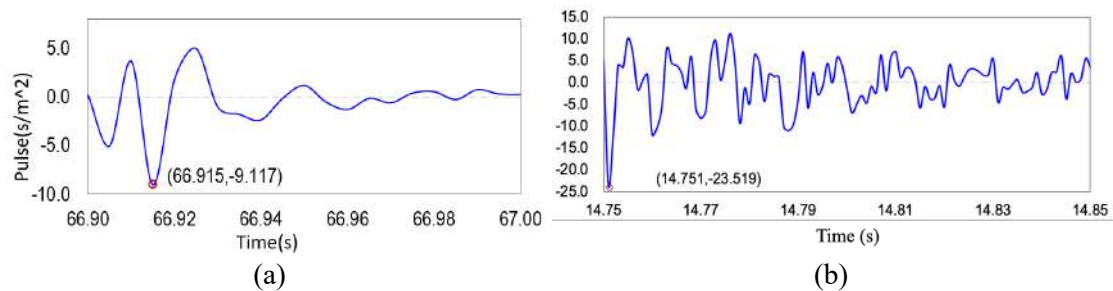


Fig. 7 Shock waves extracted from the waveforms shown in Fig. 6 for (a) shake-table test A and (b) shake-table test B.

### 3. Generating a training database

#### 3.1 Nonlinear response of single-degree-of-freedom system

As a training database, 20,000 response acceleration waveforms were generated using nonlinear analysis of single-degree-of-freedom models. As shown in the flowchart shown in Fig. 8, 18 waves for aseismic design of structures were randomly selected, their amplitudes were increased by 0.1 in the range of 0.1 to 1.5. Response analysis was performed using a bilinear model. Calculate the initial shear stiffness by randomly selecting the natural period of the model within the range of 0.3 s to 2.0 s. The yield force is 0.2 to 1.2 times



the mass, and the yield displacement is calculated by the ratio of the yield force to the shear stiffness. The stiffness after yielding varies between 0.1 and 0.6 times of the initial stiffness.

### 3.2 Noise simulation (database without beam-end fracture)

In the actual measurement, noises were mixed to the records due to ambient environmental vibration, human activity, and the performance of measuring equipment and so on. If the ratio of noise to signal is large, valuable information in the signal may not be recognized. Therefore, it is necessary to consider the effect of noise in training to recognize the characteristics of beam-end fractures. In this study, a uniform noise distribution was applied to the response acceleration waveform of the single-degree-of-freedom system in the amplitude range of  $-0.25 \text{ m/s}^2$  to  $0.25 \text{ m/s}^2$ . Noise was added to the 20,000 acceleration response waveforms generated by the nonlinear numerical analysis, half of which were used as training data for "no beam-end fracture".

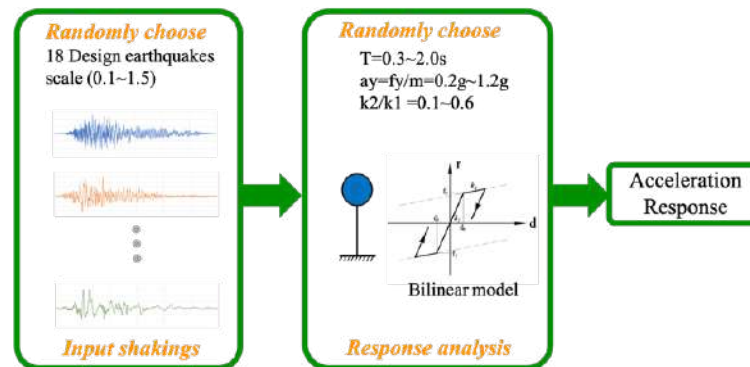


Fig. 8 Flow chart and parameters of the single-degree-of-freedom model for numerical generation of data base of response acceleration waveforms.

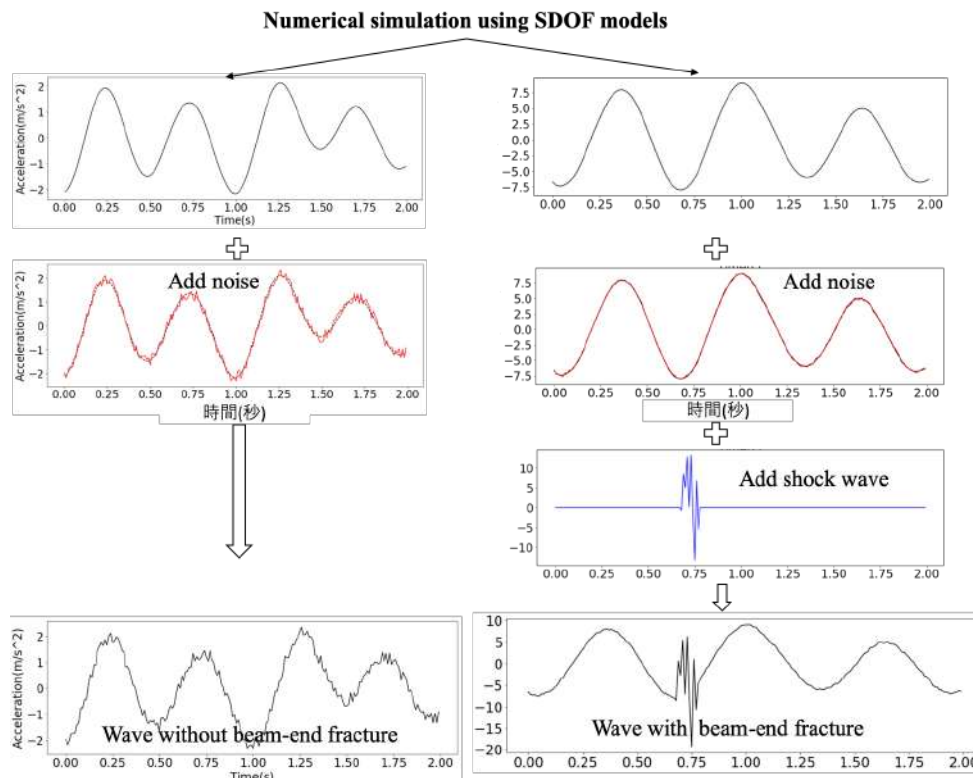


Fig. 9 Flow of training data creation without beam-end fracture (left) and with beam-end fracture (right).



### 3.3 Motion wave simulation (database with beam-end fracture)

In order to recognize the characteristics of the shock waves generated by the beam-end fracture by the neural network. Shock waves were added to the remained 10,000 noise-added acceleration responses to generate the training data with beam-end fracture. The maximum amplitude of the shock wave is limited to be within 1.5 times of the maximum amplitude of the response acceleration. Since the beam-end fracture occurs instantaneously, the length of the shock wave was set to be 0.1 s. At the time of training, every 200 data were identified. Fig.9 shows the flow of generating training databases for "without beam-end fracture" and "with beam-end fracture".

## 4. Construction, training and verification of convolutional neural network (CNN)

### 4.1 Construction of CNN model

Fig. 10 shows the configuration of the CNN model used in this study. The first layer is an input layer for training data. Three 1D Convolution-ReLU (one-dimensional convolution-rectifying linear unit) layers are stacked, followed by a pooling layer. This pattern is repeated until the input data is merged into a spatially smaller size. Then the matrix is flattened to a 1D vector containing elements. Finally, in the softmax layer, it is determined whether each input data is "without beam-end fracture" or "with beam-end fracture". The last layer is the output layer. It is responsible for outputting the class corresponding to the maximum probability. This deep CNN has a total of 408,322 parameters and 12 hidden layers.

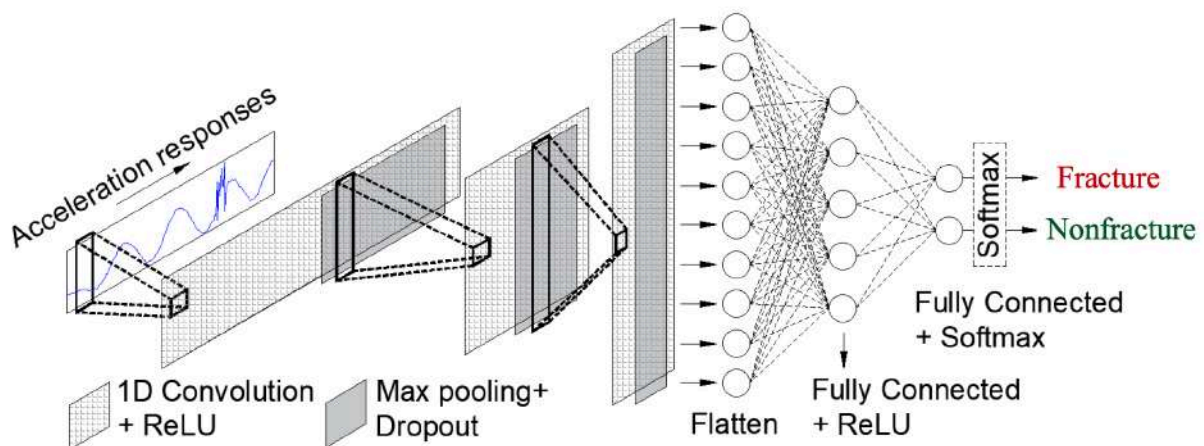


Fig. 10 Configuration of convolutional neural network

### 4.2 CNN training

Training a CNN model is the process of finding the optimal variable configuration for the CNN model, and finds two types of configuration variables that contribute in different ways to the learning process.

#### 1. Parameters of CNN model

The values of configuration variables inside the model (eg, weights of artificial neural networks, support vectors of support vector machines, coefficients for linear or logistic regression, etc.) can be derived from training<sup>[4]</sup>. However, they are stored as part of the trained model and cannot be set manually.

#### 2. Hyperparameters



Hyperparameters are set before the learning process begins and cannot be derived from training. The time required for training and testing a model depends on its hyperparameters. The hyperparameter depends on the value or the components of the model design (learning rate, dropout rate, number of hidden layers, activation function). Hyperparameters are determined by an iterative process subject to constraints such as computer configuration and time costs. The training procedure can be considered a trade-off between hyperparameters and time costs. There are two main methods for optimizing hyperparameters. Trial and error processing<sup>[5]</sup> and grid search.

i. The trial-and-error approach estimates the configuration and trains the neural network based on that configuration. Evaluate the performance of the trained neural network and repeat the search process until the best configuration is found. This approach is used first to determine the number of training data. In this study, we tried training with four kinds of data of 1000, 5000, 10000, and 15000. The number of data for "no beam end break" and "with beam end break" were the same, and the ratio of the number of training and verification data was set to 4: 1. The results of the training and verification are shown in Fig.11. Overfitting occurred when the number of training data was 1000. As the number of training data sets increases, the accuracy and loss curves become more stable, and as the number of training data increases to 15,000, more than 90% accuracy can be ensured. In this study, we used 20,000 training data, so the accuracy is sufficient.

ii. A grid search is an exhaustive search in a manually specified hyperparameter subspace. The learning rate, batch size, and epoch that need to be adjusted for good performance are selected by grid search from a reasonable set of values for each hyperparameter. In this study, as the setting that achieved the highest score in the verification procedure, we output a result with a learning rate of  $1e-05$ , a batch size of 16, and an epoch of 20 with an accuracy of 0.9999375.

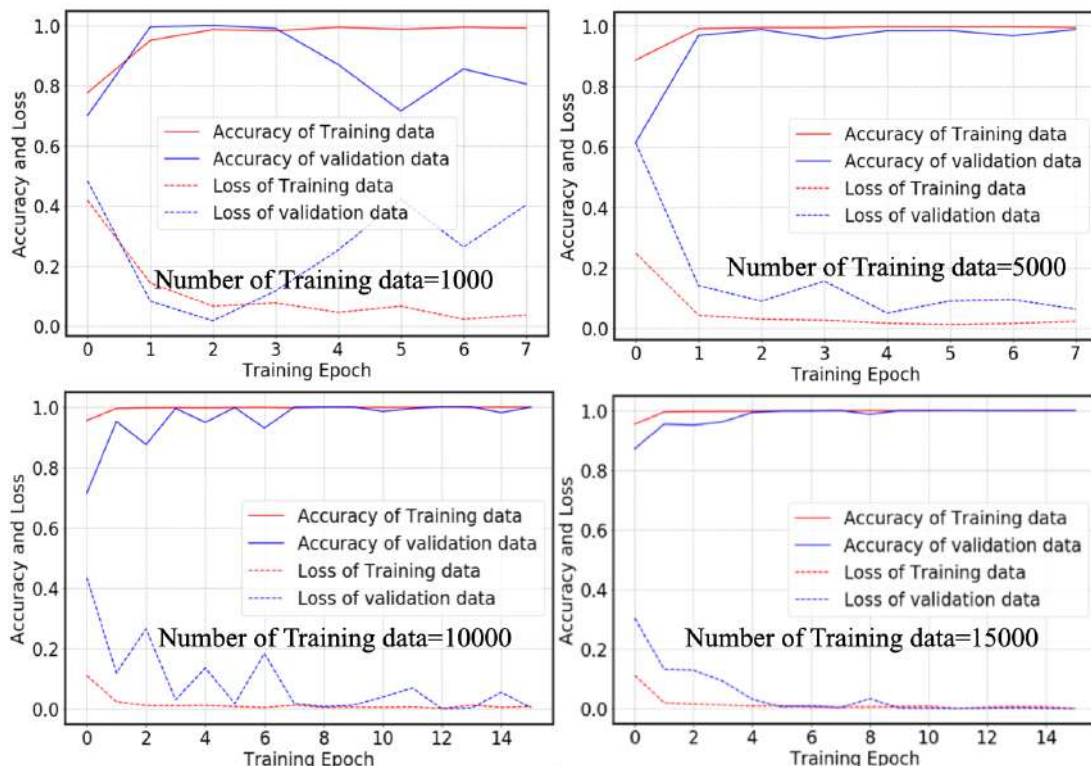


Fig. 11 Training verification based on training data volume





### 4.3 Verification of trained CNN

#### 4.3.1 Verification using simulated waveforms

To examine the performance of the trained CNN model, we first verify it using 200 simulated waveforms. The ratio of the data of "no beam-end fracture" (positive) and "with beam-end fracture" (negative) is 1:1. The predicted class is compared with the true class to calculate the accuracy given by the confusion matrix. TP (True Positive) was given to CNN when it was correctly judged to be correct. FN (False Negative) is the case that "positive example" is incorrectly determined as "negative example. FP (False Positive) is corresponding to the case that "negative example" is incorrectly determined as "positive example", while TN (True Negative) is for the case that "negative example" is correctly determined. The overall accuracy is defined as the Eq. (1). The result of the verification using the simulated waveforms is shown in Figure 12(a). As a result, the verification accuracy using simulated data was as high as 100%.

$$\text{Accuracy} = (TP + TN) / (TP + FP + FN + TN) \quad (1)$$

#### 4.3.2 Verification using shaking table test data

Using the shaking table test data of two steel-framed buildings performed by E-Defense, 80 one-second verification data were created to verify the performance of the trained CNN model. These 80-verification data were previously classified into "no beam-end fracture" and "with beam-end fracture". In the evaluation process, as in the method described in the previous section, Fig. 11(b) shows the results of comparing the prediction class of 80 pieces of verification data with the true class and calculating the accuracy using the confusion matrix. Judgment was performed with 100% accuracy for data with beam end breaks and 97.5% for data without beam end breaks. In other words, as a result of verification using actual data, the verification accuracy was 97.5%.

		Predicted class		Per-class accuracy
		Fracture	Nonfracture	
Actual class	Fracture	100	0	100%
	Nonfracture	0	100	100%
Total accuracy				100%

(a)

		Predicted class		Per-class accuracy
		Fracture	Nonfracture	
Actual class	Fracture	40	0	100%
	Nonfracture	1	39	97.5%
Total accuracy				98.75%

(b)

Fig. 12 Verification results using (a) simulated waveforms and (b) shaking table test data.

## 5. Conclusions and future work

In this study, we proposed a method to detect beam-end fractures of steel structures directly from acceleration data using convolutional neural network (CNN). The CNN model was trained by amount of noise-added data of the nonlinear response analysis using the one-degree-of-freedom system and the shock-wave-added waveforms. The number of the training data was 200, and the grid search method was used for



the training process to find the best hyperparameter configuration. The accuracy of the trained CNN model was verified using 200 simulation data and 80 shaking table test data, and as a result, both were evaluated with high accuracy. The proposed method can directly recognize the shock waves caused by beam-end fracture from the acceleration waveforms.

As the future work, we will introduce the trained CNN model to smart devices, and develop a system for real-time data acquisition, analysis, storage, and transmission to the cloud using the built-in MEMS sensors in the smart devices <sup>[5],[6]</sup>. This system can be installed at the important column-beam joints of the building structures to detect beam-end fractures in real time. After the earthquakes, it is expected to be useful for decision making on the safety of the building structure and the possibility of continuous use.

#### 4. Acknowledgements

This research is a development of the Japan Society for the Promotion of Science Grant-in-Aid for Scientific Research, Young Researcher (A) "Building a one-dimensional shear beam model of building based on nonlinear wave theory and applying it to damage prediction" (Project number: 17H04732) .

#### 5. References

- [1] Cabinet Office, Government of Japan, Outline and damage situation of the Great Hanshin-Awaji Earthquake, 2006.
- [2] National Research Institute for Earth Science and Disaster Resilience (NIED), Kobe University. Experimental Study on Seismic Safety Measures of Steel Buildings Damaged under Earthquake, 2014.
- [3] Ministry of Education, Culture, Sports, Science and Technology (MEXT), Kyoto University. Research and development on quantification of collapse margin in high-rise buildings, 2014.
- [4] Kubota J, Takahashi M, Suzuki Y, Sawamoto Y, Koetaka Y, Iyama J, and Nagae T (2018), Collapse behavior of 18-story steel moment frame on shaking table test under long period ground motion, *J. Struct. Constr. Eng.*, Vol.83, No.746, pp. 625-635.
- [5] Morgenthal, G., Hopfner, H. The application of smartphones to measuring transient structural displacements. *Journal of Civil Structural Health Monitoring*, DOI: 10.1007/s13349-012- 0025-0, 2012.
- [6] Shrestha A, Dang J, Wang X (2018). Development of a smart-device-based vibration-measurement system: Effectiveness examination and application cases to existing structure. *Struct Control Health Monit.* 25:e2120. <https://doi.org/10.1002/stc.2120>.